DNA-modified nanocrystalline diamond thin-films as stable, biologically active substrates

WENSHA YANG[1], ORLANDO AUCIELLO[2], JAMES E. BUTLER[3], WEI CAI[1], JOHN A. CARLISLE[2], JENNIFER E. GERBI[2], DIETER M. GRUEN[2], TANYA KNICKERBOCKER[1], TAMI L. LASSETER[1], JOHN N. RUSSELL, JR.[3], LLOYD M. SMITH[1] AND ROBERT J. HAMERS*[1]

[1]Department of Chemistry, University of Wisconsin-Madison, 1101 University Avenue, Madison, Wisonsin 53706, USA
[2]Materials Science Division, Argonne National Laboratory, 9700 S. Cass Avenue, Argonne, Illinois 60439, USA
[3]Naval Research Laboratory, 4555 Overlook Avenue, SW Washington, DC 20375, USA
*e-mail: rjhamers@facstaff.wisc.edu

Published online: 24 November 2002; doi:10.1038/nmat779.

Diamond, because of its electrical and chemical properties, may be a suitable material for integrated sensing and signal processing. But methods to control chemical or biological modifications on diamond surfaces have not been established. Here, we show that nanocrystalline diamond thin-films covalently modified with DNA oligonucleotides provide an extremely stable, highly selective platform in subsequent surface hybridization processes. We used a photochemical modification scheme to chemically modify clean, H-terminated nanocrystalline diamond surfaces grown on silicon substrates, producing a homogeneous layer of amine groups that serve as sites for DNA attachment. After linking DNA to the amine groups, hybridization reactions with fluorescently tagged complementary and non-complementary oligonucleotides showed no detectable non-specific adsorption, with extremely good selectivity between matched and mismatched sequences. Comparison of DNA-modified ultra-nanocrystalline diamond films with other commonly used surfaces for biological modification, such as gold, silicon, glass and glassy carbon, showed that diamond is unique in its ability to achieve very high stability and sensitivity while also being compatible with microelectronics processing technologies. These results suggest that diamond thin-films may be a nearly ideal substrate for integration of microelectronics with biological modification and sensing.

A desire to integrate biomolecules with microelectronics for integrated sensing and signal processing is fuelling interest in chemical and biological modification of the group IV semiconductors[1–8]. One of the biggest challenges for integrating microelectronics and biotechnology is the need to develop interfaces that are compatible with microelectronics processing methods, and that also provide the requisite selectivity and stability when exposed to biological environments. Although microelectronic-compatible materials such as silicon, glass and gold can be biologically modified, degradation of the interfaces has been a persistent problem, inhibiting the development of integrated biological sensors. Diamond is especially attractive because, in addition to having good electrical[9,10] and chemical properties[2,3], it is widely considered to be biocompatible[8,11,12], and can be deposited as a robust, thin film on silicon and other microelectronic-compatible substrates[13–17] at moderate temperatures that are compatible with microelectronics processing[17]. Because the growth rate of diamond is very slow, economic factors favour the use of extremely thin films. To achieve very thin, continuous films, the nucleation density during growth must be extremely high, producing diamond films with crystallites of nanometre dimensions[15,16]. Here, we present a method for functionalization of nanocrystalline diamond films of submicrometre thickness, and we show that this method allows these films to act as robust, highly selective substrates for biological modification. Our results show that DNA-modified diamond thin-films exhibit extremely good selectivity, and, more importantly, show chemical stability superior to that of alternative microelectronic-compatible substrates such as gold, glass and silicon.

Two types of thin-film diamond samples were investigated. Before growth, both types of samples were treated with nanocrystalline diamond powder in an ultrasonic bath to achieve very high nucleation densities[18]. Ultra-nanocrystalline diamond (UNCD) films[15], 0.75 μm thick, were grown on n-type Si (100) substrates at Argonne National Laboratory in a 2.45 GHz microwave plasma reactor using 1% CH_4 and 99% Ar at 150 torr pressure and 800 °C for approximately two hours. Nanocrystalline diamond (NCD) films (0.5 ± 0.2 μm thick) were grown on n-type Si (100) substrates at the Naval Research Laboratories in a 2.45 GHz microwave plasma reactor (Astex Model PDS-17) using purified hydrogen (900 s.c.c.m.) and methane (99.999%, 3 s.c.c.m.) at a total pressure of 15 torr. The samples were cleaned in a series of acid baths and then, immediately before each experiment, were exposed to a 13.56 MHz inductively coupled hydrogen plasma (15 torr) for 20 minutes at 800 °C, as described previously[19]. This procedure

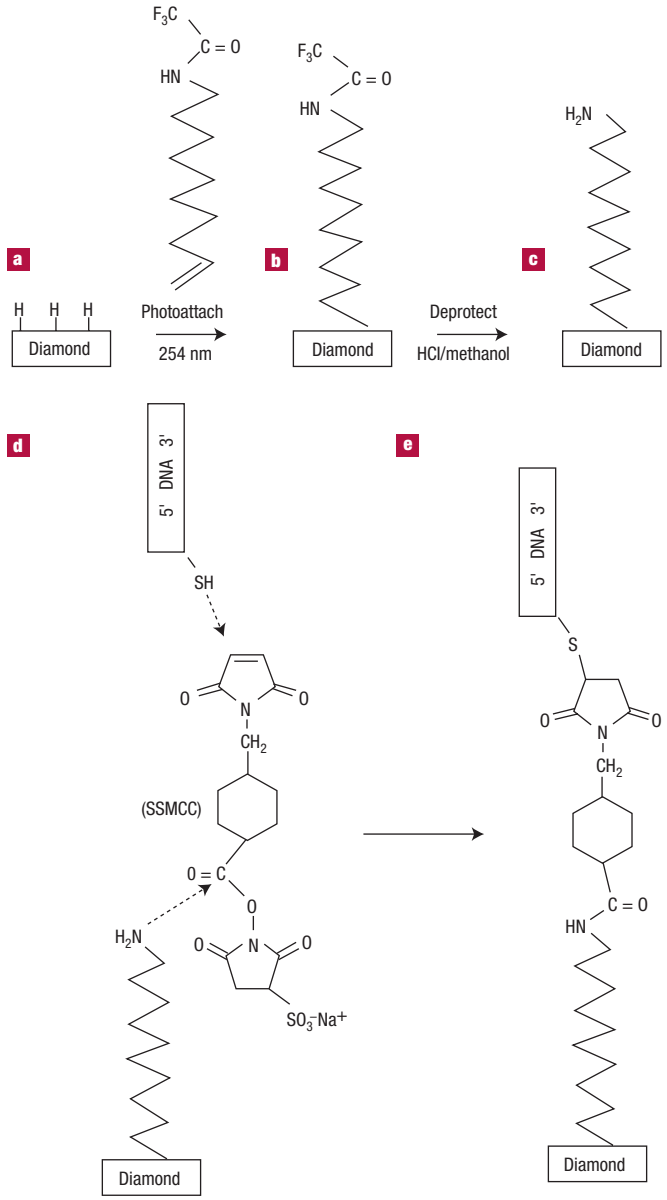

Figure 1 Sequential steps in DNA attachment to diamond thin films, as described in the text.

preferentially etches any graphitic carbon and leaves the diamond surface terminated with C-H bonds[19,20].

The DNA attachment sequence is summarized in Fig. 1. The H-terminated samples are photochemically reacted with a long-chain ω-unsaturated amine, 10-aminodec-1-ene, that has been protected with the trifluoroacetamide functional group[5]. We refer to this protected amine as TFAAD. The protected amine is then deprotected, leaving behind a primary amine (Fig. 1c). The primary amine is reacted with a heterobifunctional crosslinker sulphosuccinimidyl-4-(N-maleimidomethyl)cyclohexane-1-carboxylate (SSMCC) and finally reacted with thiol-modified DNA (Fig. 1d) to produce the DNA-modified diamond surface (Fig. 1e).

X-ray photoelectron spectroscopy (XPS) using a monochromatic Al K_α excitation source was used to characterize the chemical changes during the initial stages of modification. Figure 2a presents high-resolution C(1s), F(1s) and N(1s) spectra from a UNCD sample. Similar experiments on NCD samples (not shown) yielded nearly identical spectra. Figure 2b shows the reaction efficiency as a function of illumination time for UNCD and NCD samples exposed to TFAAD. XPS spectra of the H-terminated samples (Fig. 2a) show a single sharp C(1s) peak near 285.1 eV, and with no significant intensity at higher binding energies and no detectable amounts of fluorine or nitrogen. O(1s) spectra (not shown) reveal only a very small peak that we attribute to oxygen bonded at grain boundaries. Thus, the H-termination process leads to a well-defined starting surface for subsequent modification.

Photochemical attachment of TFAAD molecules to the surface (Fig. 1b) was accomplished by placing the sample in a nitrogen-purged reaction chamber and adding ~5 µl of TFAAD, which wets the surface with a thin, liquid film. The sample was covered with a quartz window and illuminated with a 254-nm low-pressure mercury lamp (0.35 mW cm^{-2} measured at the sample surface[21]). The F(1s) and C(1s) peak areas were used to determine the extent of surface reaction after different illumination times. Figure 2b shows that the F(1s)/C(1s) ratio ($A_{(F1s/C1s)}$) increases linearly then saturates. This time dependence can be fit with an exponential function $A_{(F1s/C1s)} = A_\infty(1-\exp^{-t/\tau})$, where t is the illumination time, τ is the characteristic reaction time at the given illumination intensity, and A_∞ is the saturation F(1s)/C(1s) XPS area ratio observed after long illumination time. This fit yields $\tau = 3.0$ hours and $A_\infty = 1.04$. Correcting the F/C area ratio for the atomic sensitivity factors (F = 1.0, C = 0.25), electron escape depth (~2 nm), and the angle of the sample normal with respect to the analyzer (45°), yields an F atom density of ~2×10^{15} F atoms cm^{-2}, or ~7×10^{14} molecules cm^{-2}. This number corresponds roughly to the number density of ~1.4×10^{15} atoms cm^{-2} on the diamond (111) surface and is consistent with formation of a dense monolayer[5,6]. A comparison of UNCD and NCD samples shows no significant difference in the rate of photochemical attachment or in the final F/C ratio. This observation suggests that the photoattachment process is relatively insensitive to the nanocrystalline grain structure of the diamond films. On the basis of the time dependence shown in Fig. 2b, all subsequent experiments reported here were performed with an exposure time of 12 hours.

Although the detailed mechanism of the photochemical reaction has not yet been fully elucidated, we determined that the absorption coefficient of the TFAAD is only 1.0 cm^{-1} at 254 nm, so that only 0.5% of the incident photons are absorbed by the ~50-µm-thick TFAAD layer. Pure, single-crystal diamond is transparent at 254 nm, and polycrystalline diamond absorbs light in the visible and near-ultraviolet regions[22]. A 0.5-µm-thick UNCD film that was removed from its silicon support by etching with a HF/HNO_3 mixture yielded an absorbance of 3.0 at 254 nm; this demonstrates that ~99.9% of the photons are absorbed within the diamond thin-film. Thus, we conclude that virtually all the ultraviolet photons are absorbed by the diamond film and not by the TFAAD liquid film. Additionally, measurements using p-polarized ultraviolet light showed that the attachment efficiency is greater when the light impinges at Brewster's angle (thereby yielding no reflection loss and complete absorption in the bulk) than at normal incidence. These results suggest that the photoattachment process involves photoexcitation of bulk electron–hole pairs, and may be similar to the mechanism recently reported for photoattachment of similar molecules on iodine-terminated silicon surfaces[23].

High-resolution spectra show the chemical changes induced by the ultraviolet light. After 12 hours of illumination, Fig. 2a shows that, in addition to the large peak at 285.1 eV (90.1% of total area, expanded off-scale) from the bulk diamond and the alkyl chain of the attached molecules, two smaller peaks having nearly equal areas are observed at 293.4 eV (4.7% of total area) and 289.0 eV (5.2% of total area). These peaks are attributed to the CF_3 group and the C=O group, respectively[6]. The F(1s) spectrum shows a single narrow peak at 689.2 eV from the

CF_3 group and the N(1s) spectrum shows a peak at 399.0 eV from the protected amine group.

After attaching the TFAAD to the surface, the amide group was deprotected by immersion in a solution of 0.36 M HCl in methanol (65 °C, 24 hours)[24]. A comparison of the XPS spectra shows that deprotection induces nearly complete (~82%) loss of the F(1s) peak at 689.0 eV and the C(1s) peak at 293.4 eV. These changes confirm loss of the CF_3 group. The N(1s) peak area broadens slightly and decreases in total area by ~10%, indicating that the amine group is intact.

Following deprotection, the samples were linked to DNA as depicted in Fig. 1d. The amine-terminated diamond surfaces were exposed to a 1.5 mM solution of SSMCC in 0.1 M triethanolamine buffer solution (pH 7) for 20 minutes, and DNA oligonucleotides (modified with a thiol group at the 5′ end) were then linked to the SSMCC-modified surface by applying 0.5 μl of 250 μM thio-oligonucleotide and keeping the sample in the humid reaction vessel for at least 6.5 hours. Experiments were conducted using two different oligonucleotides attached to the surface and using two fluorescently tagged oligonucleotides for hybridization studies. The sequences attached to the surface were 5′HS-C_6H_{12}-T_{15}- GC TTA TCG AGC TTT CG3′ (S1) and 5′HS -C_6H_{12}-T_{15}-GC TTA AGG AGC AAT CG3′ (S2). The oligonucleotides used for hybridization were modified on the 5′ end using 6-carboxy fluorescein phosphoramidite. Two complementary sequences employed were 5′-FAM-CG AAA GCT CGA TAA GC-3′ (F1, 16 bases complementary to S1 and with a four-base mismatch to S2) and 5′-FAM-CG ATT GCT CCT TAA GC-3′ (F2, 16 bases complementary to S2 and with a four-base mismatch to S1). All oligonucleotides were synthesized by the University of Wisconsin Biotechnology Center and purified by high-pressure liquid chromatography before use. In hybridization studies, 1 μl of the appropriate 5 μM oligonucleotide (F1, F2, or a mixture) was spread on the DNA-modified surface, hybridized for 20 minutes, and then washed with a standard hybridization buffer consisting of 300 mM NaCl, 20 mM sodium phosphate, 2 mM EDTA, and 6.9 mM sodium dodecyl sulphate[25].

Figure 3a shows three fluorescence images (black = high intensity) of a diamond surface—covalently modified at one location with sequence S1 and at another location with S2—after exposure to the oligonucleotides F1, F2 and a mixture. After exposure to F1, a clear single spot appears at the location of S1, indicating that the applied F1 efficiently hybridized to its complement, S1. However, there is no detectable hybridization between F1 and the four-base mismatch (S2). After this image was obtained, the sample was denatured in 8.3 M urea, rinsed in deionized water, and a second experiment was performed in which sequence F2 was applied to the surface for 20 minutes. The resulting fluorescence image shows increased fluorescence intensity only at the second spot. Figure 3b presents these data in a more quantitative way by showing the variations in intensity along a specified line. Finally, the sample was denatured again and a mixture of F1 and F2 was applied to the surface. As expected, the fluorescence image (Fig. 3a) shows hybridization at both locations.

To quantitatively evaluate the selectivity of hybridization, the average and standard deviation of the fluorescence intensity were measured in specific regions of the sample. The average fluorescence intensity from an area of 0.42 mm^2 (encompassing ~50% of the area of the hybridized spots) was 2,436 (σ = 144) for the perfect match (F2 + S2) and 525 (σ = 38) for the four-base mismatch (F2 + S1). The background in the non-functionalized region also was 525 (σ = 38). Thus, the signal from the mismatched sequence is indistinguishable from the background, whereas the perfect match yields a signal-to-noise ratio (intensity due to hybridization divided by the pooled standard deviation) of 12.9 from this 0.42 mm^2 area. Similar measurements on an NCD sample produced a signal level of 862 (σ = 66) for a perfect match, and 284 (σ = 38) for the background, yielding a signal-to-noise of 7.6. Our results indicate a slightly higher signal-to-noise ratio for UNCD diamond. However, this difference may be related to the different film thickness and needs to be explored more systematically before any clear conclusion could be drawn. For both UNCD and NCD diamond, our experiments show that DNA-modified diamond thin-films exhibit a strong preference for binding to complementary versus non-complementary sequences.

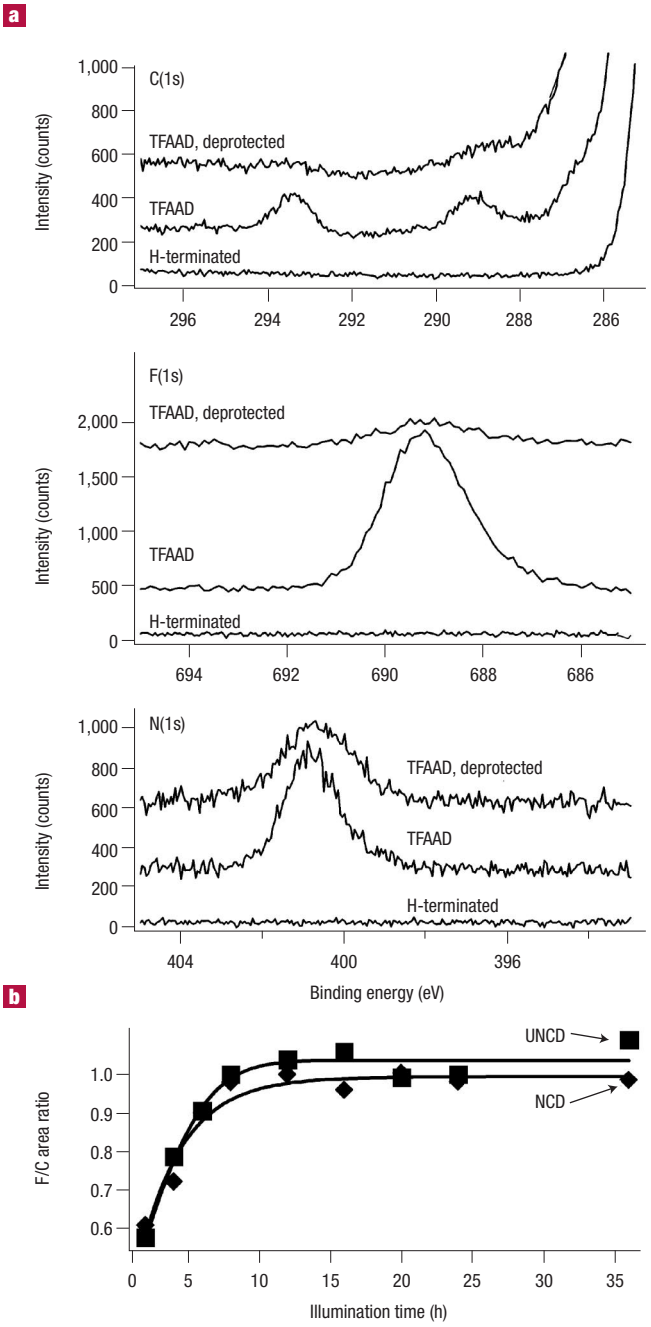

Figure 2 a, X-ray photoelectron C(1s), F(1s) and N(1s) spectra of UNCD diamond sample. Spectra shown include the clean, H-terminated surface, the same sample after photochemical attachment of the protected amine TFAAD, and after deprotection to form the primary amine. **b**, Comparison of the F(1s)/C(1s) area from UNCD and NCD samples after exposure to TFAAD and illuminated for various lengths of time.

One of the potential advantages of diamond over alternative materials is that it provides extremely good stability and is fully

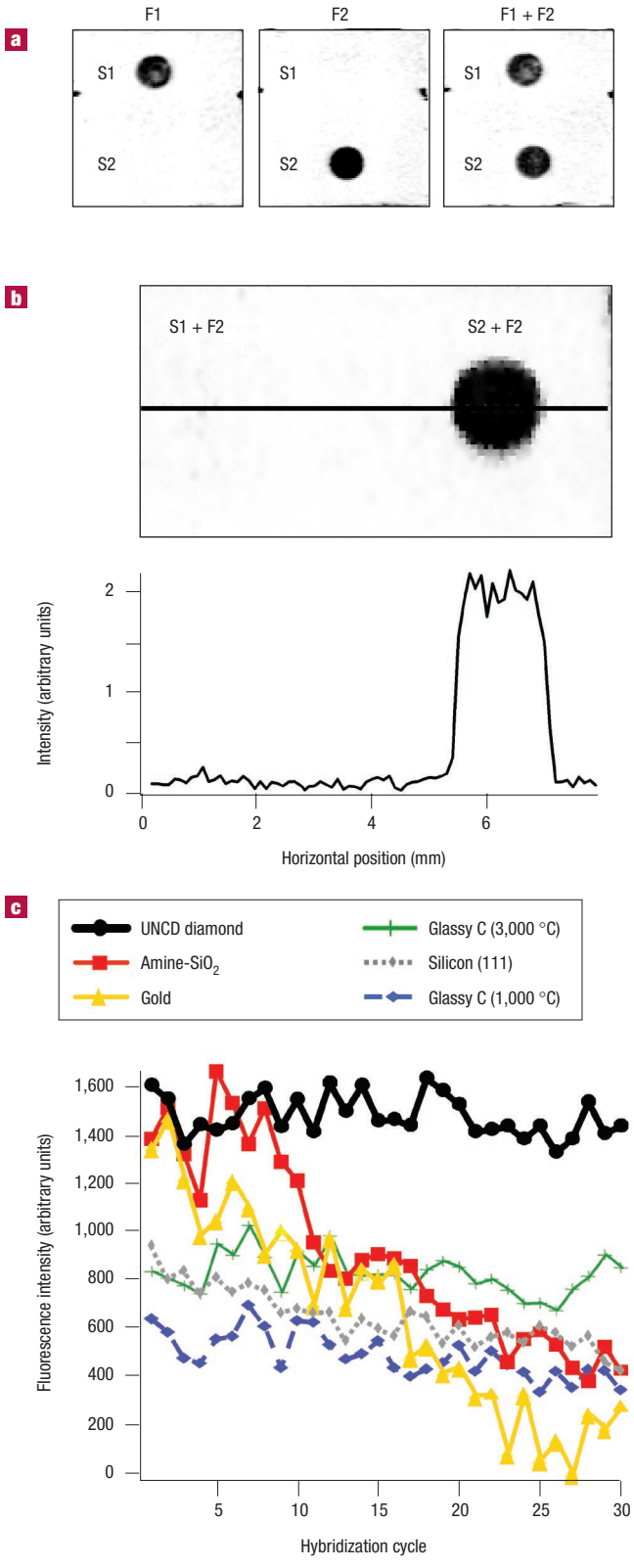

compatible with microelectronics processing methods. To demonstrate this, we performed stability studies of DNA-modified surfaces of diamond and a number of other materials including silicon, gold, a commercially available amine-terminated glass, and two types of glassy carbon. In each case, the surfaces were terminated with amine groups, reacted with SSMCC, and then with thiol-terminated DNA as described below. Corning GAPS II amine-terminated glass slides were functionalized using a 1 mM solution of SSMCC in TEA buffer (pH = 7) for 20 minutes, reacted with 250 μM DNA thio-oligonucleotide for 12 hours, and then rinsed in water and placed in TEA buffer, pH 7.0 at 37 °C for one hour to remove excess DNA. DNA-modified gold surfaces were prepared taking ozone-cleaned Au surfaces, rinsing in water then ethanol, and reacting with 11-amino-1-undecanethiol hydrochloride for 18 hours to produce amine-terminated layers. These were then rinsed successively with distilled water and ethanol, reacted with SSMCC for 20 minutes, and exposed to DNA thio-oligonueotides for 12 hours, as described previously[25]. Glassy carbon samples were cleaned and functionalized following a procedure identical to that used to modify the diamond samples as described above. Silicon(III) was funcionalized with DNA as described previously[6].

All the modified sample surfaces therefore involve nearly the same covalent chemistry. Each DNA-modified sample was then subjected to 30 successive cycles in which it was hybridized as above, the fluorescence image was obtained, the sample was denatured, rinsed and the fluorescence image was measured again. As shown in Fig. 3c, these repetitive measurements show that DNA-modified ultra-nanocrystalline diamond surfaces exhibit no measurable decrease in signal intensity even after 30 cycles. DNA-modified silicon surfaces show a small but steady decrease, consistent with previous studies[6,7,26]. DNA-modified gold surfaces degrade rapidly due to the facile hydrolysis of the thiol group under basic conditions, and even the amine-terminated glass shows rapid degradation. Two types of commercially available glassy carbon were also investigated; these differ in the temperature at which they are fabricated. Glassy carbon prepared by heating to 1,000 °C showed a ~30% degradation over 30 hybridization-denaturation cycles. A glassy carbon sample that was fabricated at a temperature of 3,000 °C showed improved stability, with little or no degradation over the course of the experiment. However, the temperature involved in fabricating glass carbon of this type is above the melting point of silicon, hence, this type of glassy carbon cannot be integrated with silicon microelectronics technology.

Because all of the DNA-modified surfaces were prepared with nearly identical chemistry, the differences in stability can be ascribed to differences in the intrinsic stability of the starting surfaces to various degradation processes. For example, it is widely recognized that gold-thiol bonds are very susceptible to oxidation, leading to solubilization of the attached layers[27]. Similarly, the degradation of chemically modified surfaces involving Si-O linkages, especially under basic conditions, is well-known[28,29]. Because oxidation of silicon is catalysed by amines[30], both crystalline silicon and SiO_2 surfaces are susceptible to amine-induced degradation[26,28,29]. In contrast, the DNA-modified diamond

Figure 3 a, Images showing fluorescence on hybridization of fluorescently labelled DNA (sequences F1 and F2) to two difference sequences of DNA (S1 and S2) bonded to UNCD diamond surface. (See text for discussion.) **b**, Variation in fluorescence intensity along the indicated line after a diamond surface modified with sequences S1 and S2 was hybridized with sequence F2. **c**, Stability of DNA-modified UNCD diamond and other materials during 30 successive cycles of hybridization and denaturation. In each case, the substrates were amine-modified and then linked to thiol-terminated DNA using SSMCC as a covalent linker (see text). The florescence intensities after hybridization with perfectly matched, fluorescently labelled complements are shown. For each substrate, the fluorescence was measured after each denaturation step and was confirmed to be zero.

surfaces clearly exhibit extremely good stability. Moreover, this is accomplished without loss of selectivity: the selectivity of binding to perfectly-matched and mismatched sequences was also investigated at the end of the 30-cycle stability test and showed no decrease in intensity from a complementary sequence, and no increased background after exposure to a non-complementary sequence.

The above experiments demonstrate that a thin film of nanocrystalline diamond, even of submicrometre thickness, can be used as a highly stable substrate for selective biological modification and adsorption. Diamond is unique in its ability to achieve high selectivity and high stability, while also being able to be prepared under conditions that are compatible with microelectronics fabrication. This combination of properties provides a unique opportunity for integration of DNA and other biological materials with microelectronics, and may enable the development of completely integrated bioelectronic sensing systems.

Received 11 July 2002; accepted 30 October 2002; published 24 November 2002.

References

1. Buriak, J. M. Organometallic chemistry on silicon and germanium surfaces. *Chem. Rev.* **102,** 1271–1308 (2002).
2. Wei, J., Smentkowski, V. S. & Yates, J. T. Jr. Diamond surface chemistry. 2. Selected bibliography. *Crit. Rev. Surf. Chem.* **5,** 73–248 (1995).
3. Bousse, L., de Rooij, N. F. & Bergveld, P. Operation of chemically sensitive field-effect sensors as a function of insulator-electrolyte interface. *IEEE Trans. Electron Dev.* **30,** 1263–1270 (1983).
4. Linford, M. R., Fenter, P., Eisenberger, P. M. & Chidsey, C. E. D. Alkyl monolayers on silicon prepared from 1-alkenes and hydrogen-terminated silicon. *J. Am. Chem. Soc.* **117,** 3145–3155 (1995).
5. Strother, T. *et al.* Photochemical functionalization of diamond films. *Langmuir* **18,** 968–971 (2002).
6. Strother, T., Cai, W., Zhao, X., Hamers, R. J. & Smith, L. M. Synthesis and characterization of DNA-modified silicon (111) surfaces. *J. Am. Chem. Soc.* **122,** 1205–1209 (2000).
7. Strother, T., Hamers, R. J. & Smith, L. M. Covalent attachment of oligodeoxyribonucleotides to amine-modified Si (001) surfaces. *Nucleic Acids Res.* **28,** 3535–3541 (2000).
8. Mathieu, H. J. Bioengineered material surfaces for medical applications. *Surf. Interface Anal.* **32,** 3–9 (2001).
9. Granger, M. C. *et al.* Standard electrochemical behavior of high-quality, boron-doped polycrystalline diamond thin-film electrodes. *Anal. Chem.* **72,** 3793–3804 (2000).
10. Swain, G. M. & Ramesham, M. The electrochemical activity of boron-doped polycrystalline diamond thin-film electrodes. *Anal. Chem.* **65,** 345–351 (1993).
11. Cui, F. Z. & Li, D. J. A review of investigations on biocompatibility of diamond-like carbon and carbon nitride films. *Surf. Coat. Technol.* **131,** 481–487 (2000).
12. Tang, L., Tasi, C., Gerberich, W. W., Kruckeberg, L. & Kanie, D. R. Biocompatibilitiy of chemical-vapor-deposited diamond. *Biomaterials* **16,** 483–488 (1995).
13. Rotter, S. Applications of conformal CVD diamond films. *Israel J. Chem.* **38,** 135–140 (1998).
14. May, P. W. Diamond thin films: a 21st-century material. *Phil. Trans. R. Soc. Lond. A* **358,** 473–495 (2000).
15. Gruen, D. M. Nanocrystalline diamond films. *Ann. Rev. Mater. Sci.* **29,** 211–259 (1999).
16. Butler, J. E. & Windischmann, H. Developments in CVD-diamond synthesis during the past decade. *Mater. Res. Bull.* **23,** 22–27 (1998).
17. Corrigan, T. D., Krauss, A. R., Gruen, D. M., Auciello, O. & Chang, R. P. H. Low temperature growth of ultrananocrystalline diamond on glass substrates for field emission applications. *Mater. Res. Soc. Symp. Proc.* **593,** 233–236 (2000).
18. Liu, H. M. & Dandy, D. S. Studies on nucleation process in diamond CVD - an overview of recent developments. *Diam. Relat. Mater.* **4,** 1173–1188 (1995).
19. Thoms, B. D., Owens, M. S., Butler, J. E. & Spiro, C. Production and characterization of smooth, hydrogen-terminated diamond C(100). *Appl. Phys. Let.* **65,** 2957–2959 (1994).
20. Thoms, B. D. & Butler, J. E. HREELS and LEED of H/C(100): The 2× 1 monohydride dimer row reconstruction. *Surf. Sci.* **328,** 291–301 (1995).
21. Rahn, R. O. Potassium iodide as a chemical actinometer for 254 nm radiation: Use of iodate as an electron scavenger. *Photochem. Photobiol.* **66,** 450–455 (1997).
22. Wilks, J. & Wilks, E. *Properties and Applications of Diamond* (Butterworth-Heinemann, Oxford, 1991).
23. Cai, W., Lin, Z., Strother, T., Smith, L. M. & Hamers, R. J. Chemical modification and patterning of iodine-terminated silicon surfaces using visible light. *J. Phys. Chem. B.* **106,** 2656–2664 (2002).
24. King, S. B. & Ganem, B. Synthetic studies on Mannostatin A and its derivatives: a new family of glycoprotein processing inhibitors. *J. Am. Chem. Soc.* **116,** 562–570 (1994).
25. Frutos, A. G., Smith, L. M. & Corn, R. M. Enzymatic ligation reactions of DNA "words" on surfaces for DNA computing. *J. Am. Chem. Soc.* **120,** 10277–10282 (1998).
26. Lin, Z. *et al.* DNA attachment and hybridization at the silicon (100) surface. *Langmuir* **18,** 788–796 (2002).
27. Everett, W. R. & Fritschfaules, I. Factors that influence the stability of self-assembled organothiols on gold under electrochemical conditions. *Anal. Chim. Acta* **307,** 253–268 (1995).
28. Gray, D. E., Case-Green, S. C., Fell, T. S., Dobson, P. J. & Southern, E. M. Ellipsometric and interferometric characterization of DNA probes immobilized on a combinatorial array. *Langmuir* **13,** 2833–2842 (1997).
29. Major, R. C. & Zhu, X.-Y. Two-step approach to the formation of organic monolayers on the silicon oxide surface. *Langmuir* **17,** 5576–5580 (2001).
30. Finne, R. M. & Klein, D. L. A water-amine complexing agent system for etching silicon, *J. Electrochem. Soc.* **114,** 965–970 (1967).

Acknowledgements

The authors acknowledge the assistance of Thomas Beebe and Matthew Wells. This work was supported in part by the US Office of Naval Research N00014-01-1-0654, the Wisconsin Alumni Research Foundation, the National Institutes of Health Grant R01 EB00269, the National Science Foundation and the US Department of Energy, BES-Materials Sciences, under Contract W-31-109-ENG-38. Correspondence and requests for materials should be addressed to R.J.H.

Competing financial interests

The authors declare that they have no competing financial interests.